

## Experimental investigation on mechanical behavior of geopolymer light weight concrete

Suresh Kumar Paramasivam<sup>1</sup> , Suganya Rajendran<sup>2</sup>

<sup>1</sup>University College of Engineering, Department of Civil Engineering, 607106, Panruti, Tamil Nadu, India.

<sup>2</sup>University College of Engineering, Department of Civil Engineering, 621731, Ariyalur, Tamil Nadu, India.

e-mail: erpsuresh@rediffmail.com, sugansemier@gmail.com

### ABSTRACT

The development of lightweight geopolymer concrete is the main goal of this research work, and the outcomes were evaluated in comparison to the control mix. In this work, geopolymer concrete was produced using fly ash as a binder, synthetic sand as M-sand as fine aggregate, and coconut shell as well as palm shell ash for coarse aggregate. For the purpose of selecting a mix proportion via trial mixes, an initial investigation was conducted. The quantity among binder, fine and coarse aggregate, sodium hydroxide molarity, sodium silicate: sodium hydroxide ratio, the alkaline binder ratio is some of the significant variables taken into account in the current study. Investigation of the effects of various factors on the engineering characteristics of geopolymer concrete. The trial mixes were utilized to evaluate the characteristics for geopolymer concrete with a ratio of 1: 2.36 :1.02 and a Molarity of 16 with binder ratio 0.6 The key findings of this investigation is to that the coconut shell waste and palm shell can be replaced instead of fine aggregate. In-depth research was done on the mechanical behavior with geopolymer concrete, such as the mechanical and durability characteristics with control mix.

**Keywords:** Coconut shell; palm shell; geopolymer concrete.

### 1. INTRODUCTION

One tonne in cement requires roughly two tonnes in raw ingredients, such as shale and limestone. Cement consumption must be reduced for the sake of the environment since cement manufacture contributes between 5 and 7 percent of global carbon dioxide emissions [1, 2]. [3] estimate that by 2020, cement demand will have increased from its 1990s level by 115–180 percent. This demand is anticipated to have grown by 400% by the year 2050. The concrete industry has seen rapid technological advancement during the last thirty years. Research has been done extensively to completely replace the conventional cement concrete product in order to lower CO<sub>2</sub> emissions. One of this research by [4] examines the use of geopolymer concrete, or third-generation concrete. Using this innovative method, the typical concrete component, which is widely used in the construction business, can be completely eliminated [5, 6].

In a very alkaline environment, silica and alumina dissolve, dissolved oxide minerals coagulate with gelation, and a three-dimensional network (silica-aluminates structures) is created. These are the three primary stages of the geo-polymerization process. [7–9]. The resulting chemical link enables the three basic structures to form a 3D aluminium silicate network. According to [10], the most typical structures are poly (sialate), poly (sialate-siloxo), and poly (sialate-disiloxo) [11]. The production of geopolymers involves two main procedures. The first step was to blend the materials in the proper proportions based on the desired strength. The binder, coarse aggregate, & alkaline activators must all be combined in this process. The following step involves thermal curing. Many agricultural waste products, including date seedlings, oil palm shells, rubber seedlings, corn cubes, coconut shells, and periwinkle seeds, are used as alternatives to traditional aggregate, depending on availability, according to [12].

In a very alkaline environment, silica and alumina dissolve, dissolved oxide minerals coagulate with gelation, and a three-dimensional network (silica-aluminates structures) is created. These are the three primary stages of the geo-polymerization process. The resulting chemical link enables the three basic structures to form a 3D aluminium silicate network. According to [13] the most typical structures are poly (sialate), poly (sialate-siloxo), and poly (sialate-disiloxo). By polymerizing silicon, aluminium, and oxygen-containing molecules

from an amorphous three-dimensional structure, geopolymers, a new class of materials, are created. The source material plus alkaline activator liquid are the two major components of geopolymers. Alumina-silicate-based geopolymers source materials should be abundant in silica and aluminium. The production of geopolymers involves two main procedures. The first step was to blend the materials in the proper proportions based on the desired strength. The binder, coarse aggregate, & alkaline activators must all be combined in this process. The following step involves thermal curing. Many agricultural waste products, including date seedlings, oil palm shells, rubber seedlings, corn cubes, coconut shells, and periwinkle seeds, are used as alternatives to traditional aggregate, depending on availability [14].

When compared to the entire world's production of coconuts, India comes in third place. The disposal of this plentiful supply of coconut shell produced by the coconut industry has a negative and significant influence on the environment [15]. By lowering this solid waste, the construction industry's use of this coconut shell will address the environmental issue there. Additionally, there is a lot of study being done on the use of coconut shells as a full or partial substitute of coarse aggregate within developing countries like India because the overall weight of concrete produced with coconut shell is less due to the unit weight for the coconut shell used inside the mixture [16].

More than 100 countries cultivate coconuts. India is third in the world for coconut output, with approximately 2 million hectares under cultivation. The Indian National Multiple Commodities Exchange estimates that 4300 nuts are produced on average per hectare, or close to 8000 million nuts annually. The Indian coconut industry, which already produces over twenty percent of all coconut oil produced worldwide, is anticipated to grow further as global demand rises. However, it is also the primary contributor to the nation's pollution issue, producing 3.18 million metric tonnes of solid garbage in the form of shells annually. In underdeveloped countries where a lot of coconut shell garbage is thrown, these wastes could be used as potential and replacement resources in the construction industry. This will reduce the price of building materials and act as a garbage disposal method, which is an advantageous arrangement [17].

## 2. MATERIALS AND METHODS

### 2.1. Material

The materials used in this experiment included water, ash from fly ashes, sodium hydroxide, sodium silicate, fine gravel (river sand), coarse gravel (blue metal), palm & coconut shells and coarse aggregate. River sand, which was accessible nearby and it is cleaned, was utilized as fine aggregate (FA). The used sand must match the requirements of IS Grade Zone-II from the 383 (1970) [18] and pass through for a 4.75 mm sieve. Sand that was used in the cementitious materials made for the current study met the aforementioned requirements and was free of silt and clay. The physical characteristics of fine aggregate are shown in Table 1.

In this experiment, coconut and palm shells are utilised in place of some of the natural coarse aggregate. The physical characteristics of these materials are provided in Table 2, and their chemical characteristics are listed in Table 3.

Fly ash belongs to Class F type both its chemical and physical properties are given in Tables 4, 5 respectively, in the experimental study. Fly ash components, which are typically round, glassy particles, rarely contain uneven or angular particles. Particles in fly ash are typically between 10- and 100-microns particle size. Fly ash is unique in that it has a low specific gravity that ranges from 2.0 - 2.6, a consistent gradation, and less flexibility when it is wet. When fly ash is not securely packed or vibrated, its bulk density varies between 540 to 850 kg/m<sup>3</sup>, while it ranges between 1120 to 1450 kg/m<sup>3</sup> as it is [19].

The chemical composition of fly ash is based on the characteristics of the coal utilised in power plants. The many different types in coal utilised by power plants result in a wide range in compositions in fly ash. Ash mostly consists of silica (SiO<sub>2</sub>), alumina (Al<sub>2</sub>O<sub>3</sub>), the iron oxide (FeO), with minor amounts of calcium (CaO), magnesium (MgO), and sulphur (SO<sub>3</sub>). The components of fly ash—silica, iron, free lime, as well as carbon—have an effect on its technical properties by Guo et al., (2012), Hardjito et al., (2012). Caustic soda is a different name for sodium hydroxide. It often comes in two main forms, flakes and pellets. It was consumed in flakes form for this study. The role of sodium hydroxide in geopolymer concrete is crucial. It serves as a geopolymer concrete activator. In accordance with the molarities, sodium hydroxide was dissolved in 1 litre of water to create sodium hydroxide solution. The workability as well as endurance of geopolymer concrete are significantly influenced by this molarity. In this work, the characteristics of geopolymer concrete at 4 distinct molarities—8M, 10M, 12M, and 16M—were determined for both the fresh and hardened states. Sodium silicate is often referred to as water glass or soluble glass [18–20]. It is a concrete accelerator. It makes up the majority of the geopolymer concrete mix. To activate the geopolymeric source materials, sodium silicate is always utilised in conjunction

**Table 1:** Physical properties of river sand.

| PHYSICAL PROPERTIES | RIVER SAND |
|---------------------|------------|
| Appearance          | Grainy     |
| Specific Gravity    | 2.73       |
| Bulk Density        | 2.75 g/cc  |
| Water Absorption    | 1.48%      |
| Moisture Content    | 1.33%      |
| Zone                | II         |
| Colour              | White      |
| Finness Modulus     | 1.5        |
| Maximum Grian Size  | 1.18       |

**Table 2:** Physical properties of coarse aggregates.

| PROPERTIES                        | COARSE AGGREGATE  | COCONUT SHELL          | PALM SHELL              |
|-----------------------------------|-------------------|------------------------|-------------------------|
| Size and Shape                    | 12.5 mm & Angular | 12.5 mm & Rough Convex | 12.5 mm & Smooth Convex |
| Specific Gravity                  | 2.65              | 1.15                   | 1.35                    |
| Water Absorption                  | 1.74              | 22                     | 12                      |
| Crushing Value (%)                | 17.54             | 2.58                   | 2.15                    |
| Impact Strength (%)               | 14.69             | 8.15                   | 4.5                     |
| Abrasion Resistance               | 26.89             | 2.23                   | 7.6                     |
| Elongation Index (%)              | 22                | 27                     | 12.36                   |
| Flackiness Index (%)              | 32                | 85                     | 37.5                    |
| Bulk Density (kg/m <sup>3</sup> ) | 1620              | 625                    | 525                     |
| Moisture Content (%)              | 0.8               | 10.33                  | 6-12                    |
| Fineness Modulus (%)              | 6.8               | 6.5                    | 6.25                    |

**Table 3:** Chemical properties of coarse aggregates.

| PROPERTIES                     | COARSE AGGREGATE | COCONUT SHELL | PALM SHELL |
|--------------------------------|------------------|---------------|------------|
| CaO                            | 13.33            | 04.98         | 12.5       |
| SiO <sub>2</sub>               | 55.7             | 20.70         | 25.1       |
| Al <sub>2</sub> O <sub>3</sub> | 0.77             | 05.75         | 7.26       |
| MgO                            | 9.58             | 01.89         | -          |
| Na <sub>2</sub> O              | 0.14             | 0.66          | -          |
| SO <sub>3</sub>                | -                | 02.75         | 1.4        |
| P <sub>2</sub> O <sub>5</sub>  | -                | 00.05         | 2.4        |
| K <sub>2</sub> O               | 0.09             | 00.15         |            |
| MnO                            | -                | 00.20         | 0.74       |
| Fe <sub>2</sub> O <sub>3</sub> | 0.37             | 02.50         | 12.5       |
| TiO <sub>2</sub>               | 0.01             | -             | 0.92       |
| CuO                            | -                | -             | 1.4        |

with sodium hydroxide. It includes a crucial step in the production of geopolymer concrete. Before casting, sodium silicate and sodium hydroxide solution are combined. In order to make alkaline activator, the solution of sodium hydroxide (NaOH) with 8–16 Molarity was mixed with sodium silicate (13% Na<sub>2</sub>O, 30% SiO<sub>2</sub>, and 57% water by mass: Na<sub>2</sub>SiO<sub>3</sub>). 24 hours before to casting, a laboratory-made solution of sodium hydroxide was produced. On the basis of weight, a ratio of 1:2.50 of sodium hydroxide with sodium silicate was used. The experiment used only potable water. The water was clear and free of impurities including grease, oil, silt, and organic debris that might interfere with the curing and concreting processes [21–23].

**Table 4:** Physical properties of fly ash.

| PROPERTIES       | VALUE                  |
|------------------|------------------------|
| Finesses modulus | 7.86                   |
| Specific gravity | 2.30                   |
| Particle Size    | 10 $\mu$ m–100 $\mu$ m |
| Specific Gravity | 2.5                    |

**Table 5:** Chemical properties of fly ash.

| CHEMICAL COMPONENTS  | MINIMUM % BY MASS<br>(IS 3812:1981) | FLY ASH (MTPP) |
|--|-------------------------------------|----------------|
| SiO <sub>2</sub> + Al <sub>2</sub> O <sub>3</sub> + Fe <sub>2</sub> O <sub>3</sub> | 70                                  | 90.5           |
| SiO <sub>2</sub>   | 35                                  | 58             |
| CaO  | 5                                   | 3.6            |
| SO <sub>3</sub>  | 2.75                                | 1.8            |
| Na <sub>2</sub> O  | 1.5                                 | 2              |
| L.O. I   | 12                                  | 2              |
| MgO  | 5                                   | 1.91           |

**Table 6:** Proportion for trail mix with blinder ratio.

| MIX ID    | MIX PROPORTION     | MOLARITY OF NaOH | BINDER RATIO | COMPRESSION STRENGTH @ 28 DAYS (N/mm <sup>2</sup> ) |
|-----------|--------------------|------------------|--------------|---|
| 1         | 1:3.24:1.45        | 8                | 0.45         | 18.75   |
| 2         | 1:3.24:1.45        | 10               | 0.45         | 19.32   |
| 3         | 1:3.24:1.45        | 12               | 0.45         | 21.57   |
| 4         | 1:3.24:1.45        | 14               | 0.45         | 23.34   |
| 5         | 1:3.24:1.45        | 16               | 0.45         | 25.56   |
| 6         | 1:2.83:1.25        | 8                | 0.50         | 22.23   |
| 7         | 1:2.83:1.25        | 10               | 0.50         | 25.21   |
| 8         | 1:2.83:1.25        | 12               | 0.50         | 26.98   |
| 9         | 1:2.83:1.25        | 14               | 0.50         | 28.56   |
| 10        | 1:2.83:1.25        | 16               | 0.50         | 30.89   |
| 11        | 1:2.55:1.10        | 8                | 0.55         | 24.61   |
| 12        | 1:2.55:1.10        | 10               | 0.55         | 26.58   |
| 13        | 1:2.55:1.10        | 12               | 0.55         | 30.63   |
| 14        | 1:2.55:1.10        | 14               | 0.55         | 32.48   |
| 15        | 1:2.55:1.10        | 16               | 0.55         | 35.26   |
| 16        | 1:2.51:1.04        | 8                | 0.60         | 33.65   |
| 17        | 1:2.51:1.04        | 10               | 0.60         | 35.07   |
| 18        | 1:2.51:1.04        | 12               | 0.60         | 36.99   |
| 19        | 1:2.51:1.04        | 14               | 0.60         | 39.24   |
| <b>20</b> | <b>1:2.51:1.04</b> | <b>16</b>        | <b>0.60</b>  | <b>41.56</b>  |
| 21        | 1:2.36:1.02        | 8                | 0.65         | 32.76   |
| 22        | 1:2.36:1.02        | 10               | 0.65         | 33.98   |
| 23        | 1:2.36:1.02        | 12               | 0.65         | 35.53   |
| 24        | 1:2.36:1.02        | 14               | 0.65         | 36.98   |
| 25        | 1:2.36:1.02        | 16               | 0.65         | 37.84   |

**Table 7:** Designed mix calculation and ratio for M1 to M30.

| MIX DESIGNATION | MIX RATIO   | MOLARITY | BINDER RATIO | % OF REPLACEMENT OF CS | % OF REPLACEMENT OF PS |
|-----------------|-------------|----------|--------------|------------------------|------------------------|
| M1              | 1:2.51:1.04 | 8        | 0.6          | 0%                     | 0%                     |
| M2              | 1:2.51:1.04 | 8        | 0.6          | 2.5%                   | 2.5%                   |
| M3              | 1:2.51:1.04 | 8        | 0.6          | 5%                     | 5%                     |
| M4              | 1:2.51:1.04 | 8        | 0.6          | 7.5%                   | 7.5%                   |
| M5              | 1:2.51:1.04 | 8        | 0.6          | 10%                    | 10%                    |
| M6              | 1:2.51:1.04 | 8        | 0.6          | 12.5%                  | 12.5%                  |
| M7              | 1:2.51:1.04 | 10       | 0.6          | 0%                     | 0%                     |
| M8              | 1:2.51:1.04 | 10       | 0.6          | 2.5%                   | 2.5%                   |
| M9              | 1:2.51:1.04 | 10       | 0.6          | 5%                     | 5%                     |
| M10             | 1:2.51:1.04 | 10       | 0.6          | 7.5%                   | 7.5%                   |
| M11             | 1:2.51:1.04 | 10       | 0.6          | 10%                    | 10%                    |
| M12             | 1:2.51:1.04 | 10       | 0.6          | 12.5%                  | 12.5%                  |
| M13             | 1:2.51:1.04 | 12       | 0.6          | 0%                     | 0%                     |
| M14             | 1:2.51:1.04 | 12       | 0.6          | 2.5%                   | 2.5%                   |
| M15             | 1:2.51:1.04 | 12       | 0.6          | 5%                     | 5%                     |
| M16             | 1:2.51:1.04 | 12       | 0.6          | 7.5%                   | 7.5%                   |
| M17             | 1:2.51:1.04 | 12       | 0.6          | 10%                    | 10%                    |
| M18             | 1:2.51:1.04 | 12       | 0.6          | 12.5%                  | 12.5%                  |
| M19             | 1:2.51:1.04 | 14       | 0.6          | 0%                     | 0%                     |
| M20             | 1:2.51:1.04 | 14       | 0.6          | 2.5%                   | 2.5%                   |
| M21             | 1:2.51:1.04 | 14       | 0.6          | 5%                     | 5%                     |
| M22             | 1:2.51:1.04 | 14       | 0.6          | 7.5%                   | 7.5%                   |
| M23             | 1:2.51:1.04 | 14       | 0.6          | 10%                    | 10%                    |
| M24             | 1:2.51:1.04 | 14       | 0.6          | 12.5%                  | 12.5%                  |
| M25             | 1:2.51:1.04 | 16       | 0.6          | 0%                     | 0%                     |
| M26             | 1:2.51:1.04 | 16       | 0.6          | 2.5%                   | 2.5%                   |
| M27             | 1:2.51:1.04 | 16       | 0.6          | 5%                     | 5%                     |
| M28             | 1:2.51:1.04 | 16       | 0.6          | 7.5%                   | 7.5%                   |
| M29             | 1:2.51:1.04 | 16       | 0.6          | 10%                    | 10%                    |
| M30             | 1:2.51:1.04 | 16       | 0.6          | 12.5%                  | 12.5%                  |

## 2.2. Mix design calculation

To achieve a compressive strength of 40 kN/m<sup>3</sup>, a light geopolymer is prepared using a number of trial mixtures. The trial mixture proportions are listed in Table 3, and in that trial, various mixtures are prepared by changing the molarity from 8 to 16 and the binder ratio of 0.45 to 0.65 are stated in Table 4. The mix ratio is chosen to be 1: 2.5: 1.04 with a 0.6 binder ratio as the ideal replacement percentage. The precise ratios of the mixed coconut and palm shells are displayed in Tables 6 and 7.

## 3. RESULTS AND DISCUSSION

### 3.1. Mechanical behavior of concrete

With an ambient curing molarity of 8M–16M, the mechanical parameters like compressive strength, split tensile strength, and flexural strength are determined. Table 8 lists the findings of the compression test, Table 9 lists the results of the split tension strength test, Table 10 lists the results of the flexural strength test, and Figure.1 lists the mechanical characteristics of geopolymer concrete. Figures 2 and 3 depict the concrete test's compressive

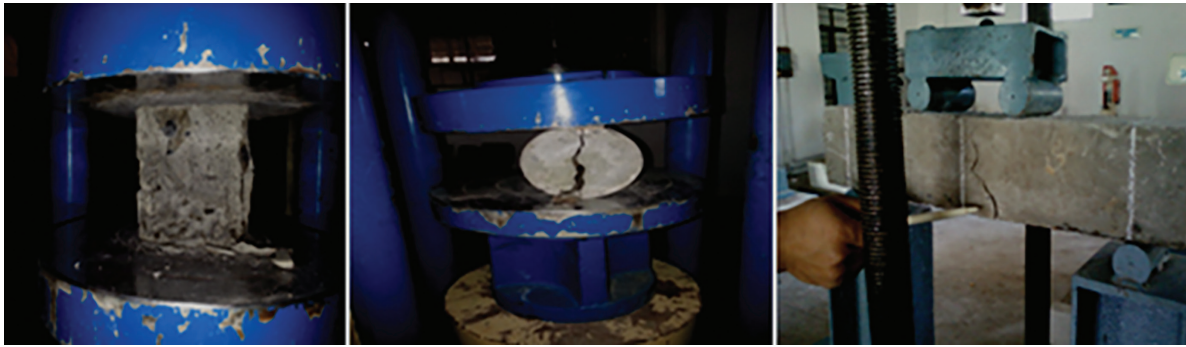


**Figure 1:** Mechanical properties test.

**Table 8:** Compression behaviour of concrete from 7 to 90 days.

| MIX ID | COMPRESSION STRENGTH @ 28 DAYS (N/mm <sup>2</sup> ) |         |         |         |         |
|--------|---|---------|---------|---------|---------|
|        | 7 DAYS  | 14 DAYS | 28 DAYS | 56 DAYS | 90 DAYS |
| M1     | 21.87   | 30.74   | 33.65   | 34.54   | 34.56   |
| M2     | 22.65   | 31.87   | 34.52   | 38.23   | 38.54   |
| M3     | 23.54   | 33.08   | 35.98   | 39.23   | 39.54   |
| M4     | 22.23   | 32.86   | 34.54   | 37.56   | 37.68   |
| M5     | 20.54   | 30.41   | 32.65   | 35.47   | 35.89   |
| M6     | 18.53   | 27.54   | 30.48   | 32.69   | 32.67   |
| M7     | 22.47   | 31.54   | 35.07   | 35.18   | 35.84   |
| M8     | 23.68   | 31.87   | 34.52   | 36.85   | 36.54   |
| M9     | 24.42   | 33.08   | 35.98   | 37.48   | 38.54   |
| M10    | 23.46   | 32.75   | 34.56   | 35.24   | 37.69   |
| M11    | 21.54   | 31.64   | 33.54   | 34.68   | 36.87   |
| M12    | 19.63   | 30.28   | 31.86   | 33.16   | 34.13   |
| M13    | 23.54   | 33.47   | 36.99   | 37.98   | 37.64   |
| M14    | 24.76   | 35.49   | 37.52   | 38.61   | 38.42   |
| M15    | 26.84   | 36.68   | 38.21   | 39.54   | 40.53   |
| M16    | 23.48   | 34.89   | 36.23   | 37.28   | 38.64   |
| M17    | 22.08   | 32.51   | 34.38   | 35.47   | 36.29   |
| M18    | 20.57   | 30.87   | 32.04   | 33.28   | 34.84   |
| M19    | 24.36   | 34.52   | 38.24   | 38.94   | 38.53   |
| M20    | 25.63   | 35.28   | 39.57   | 40.23   | 40.29   |
| M21    | 27.65   | 38.54   | 40.23   | 42.08   | 42.19   |
| M22    | 25.28   | 36.49   | 38.26   | 40.56   | 40.67   |
| M23    | 23.56   | 33.73   | 36.72   | 38.61   | 38.54   |
| M24    | 22.54   | 31.92   | 38.86   | 36.58   | 36.19   |
| M25    | 25.46   | 35.23   | 41.56   | 43.54   | 43.28   |
| M26    | 27.56   | 37.16   | 43.58   | 44.67   | 44.89   |
| M27    | 29.64   | 39.53   | 46.28   | 47.98   | 47.23   |
| M28    | 27.03   | 37.65   | 43.89   | 44.95   | 45.86   |
| M29    | 25.46   | 35.26   | 40.58   | 43.57   | 43.58   |
| M30    | 22.04   | 34.98   | 38.79   | 42.83   | 42.56   |

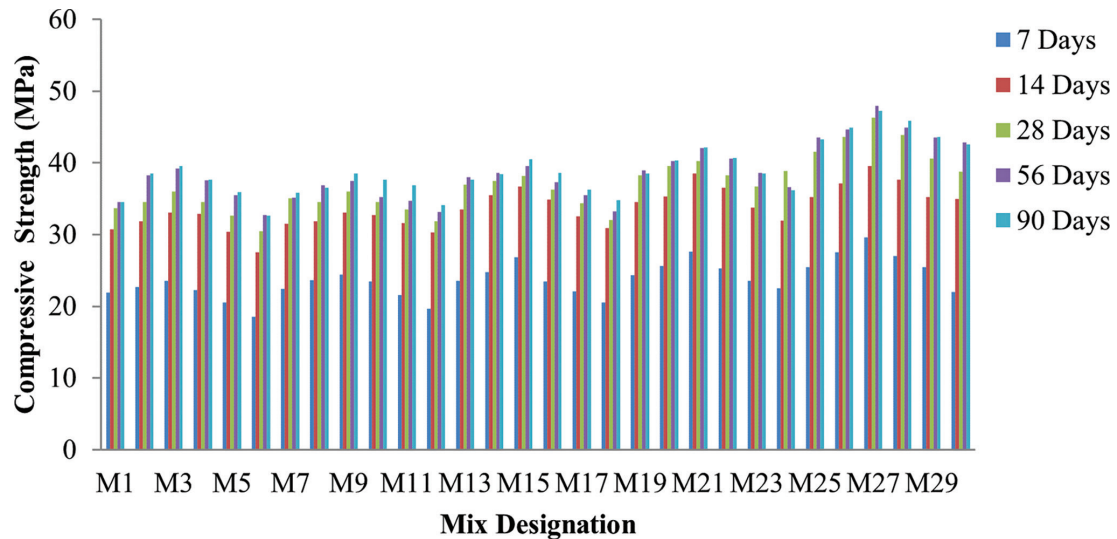


Figure 2: Graphical representation of compression strength variation from 7 to 90 days.

Table 9: Split tensile behaviour of concrete from 7 to 90 days.

| MIX ID     | SPLIT TENSILE STRENGTH @ 28 DAYS (N/mm <sup>2</sup> ) |             |             |             |             |
|------------|---|-------------|-------------|-------------|-------------|
|            | 7 DAYS  | 14 DAYS     | 28 DAYS     | 56 DAYS     | 90 DAYS     |
| M1         | 2.62  | 3.84        | 4.37        | 3.80        | 3.80        |
| M2         | 2.72  | 3.98        | 4.49        | 4.21        | 4.24        |
| M3         | 2.82  | 4.14        | 4.68        | 4.32        | 4.35        |
| M4         | 2.67  | 4.11        | 4.49        | 4.13        | 4.14        |
| M5         | 2.46  | 3.80        | 4.24        | 3.90        | 3.95        |
| M6         | 2.22  | 3.44        | 3.96        | 3.60        | 3.59        |
| M7         | 2.70  | 3.94        | 4.56        | 3.87        | 3.94        |
| M8         | 2.84  | 3.98        | 4.49        | 4.05        | 4.02        |
| M9         | 2.93  | 4.14        | 4.68        | 4.12        | 4.24        |
| M10        | 2.82  | 4.09        | 4.49        | 3.88        | 4.15        |
| M11        | 2.58  | 3.96        | 4.36        | 3.81        | 4.06        |
| M12        | 2.36  | 3.79        | 4.14        | 3.65        | 3.75        |
| M13        | 2.82  | 4.18        | 4.81        | 4.18        | 4.14        |
| M14        | 2.97  | 4.44        | 4.88        | 4.25        | 4.23        |
| M15        | 3.22  | 4.59        | 4.97        | 4.35        | 4.46        |
| M16        | 2.82  | 4.36        | 4.71        | 4.10        | 4.25        |
| M17        | 2.65  | 4.06        | 4.47        | 3.90        | 3.99        |
| M18        | 2.47  | 3.86        | 4.17        | 3.66        | 3.83        |
| M19        | 2.92  | 4.32        | 4.97        | 4.28        | 4.24        |
| M20        | 3.08  | 4.41        | 5.14        | 4.43        | 4.43        |
| M21        | 3.32  | 4.82        | 5.23        | 4.63        | 4.64        |
| M22        | 3.03  | 4.56        | 4.97        | 4.46        | 4.47        |
| M23        | 2.83  | 4.22        | 4.77        | 4.25        | 4.24        |
| M24        | 2.70  | 3.99        | 5.05        | 4.02        | 3.98        |
| M25        | 3.06  | 4.40        | 5.40        | 4.79        | 4.76        |
| M26        | 3.31  | 4.65        | 5.67        | 4.91        | 4.94        |
| <b>M27</b> | <b>3.56</b>   | <b>4.94</b> | <b>6.02</b> | <b>5.28</b> | <b>5.20</b> |
| M28        | 3.24  | 4.71        | 5.71        | 4.94        | 5.04        |
| M29        | 3.06  | 4.41        | 5.28        | 4.79        | 4.79        |
| M30        | 2.64  | 4.37        | 5.04        | 4.71        | 4.68        |

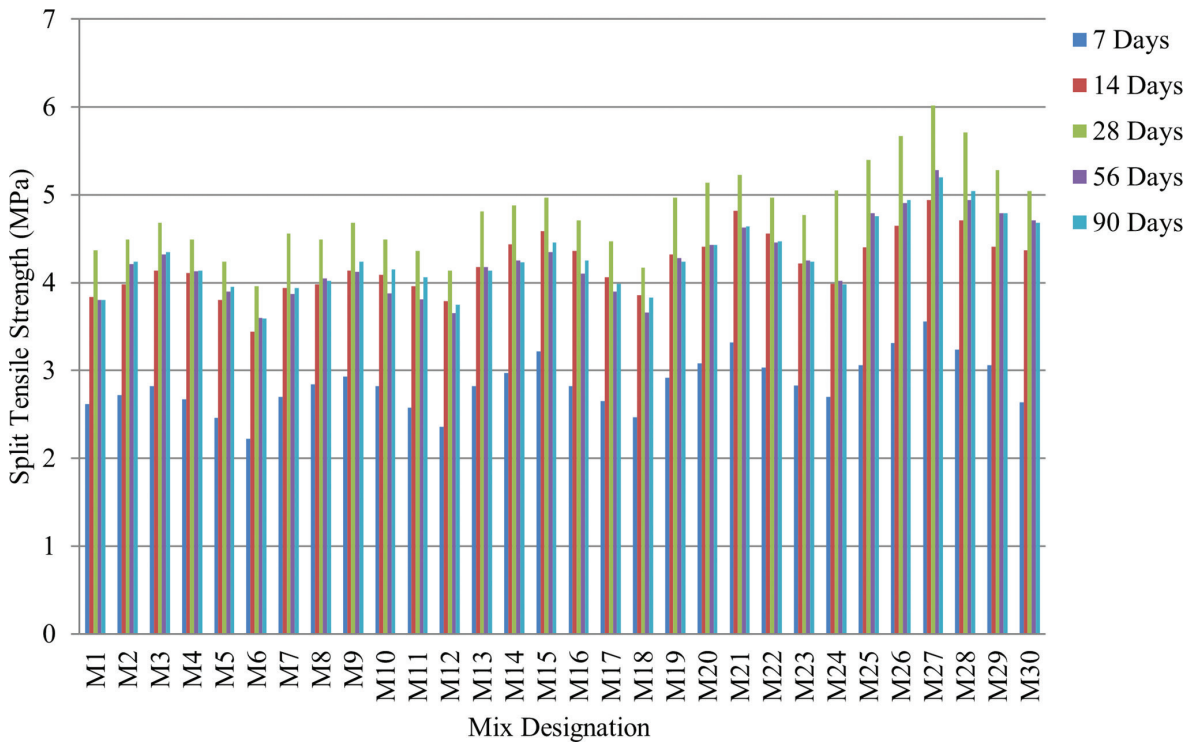


Figure 3: Graphical representation of split tensile strength variation from 7 to 90 days.

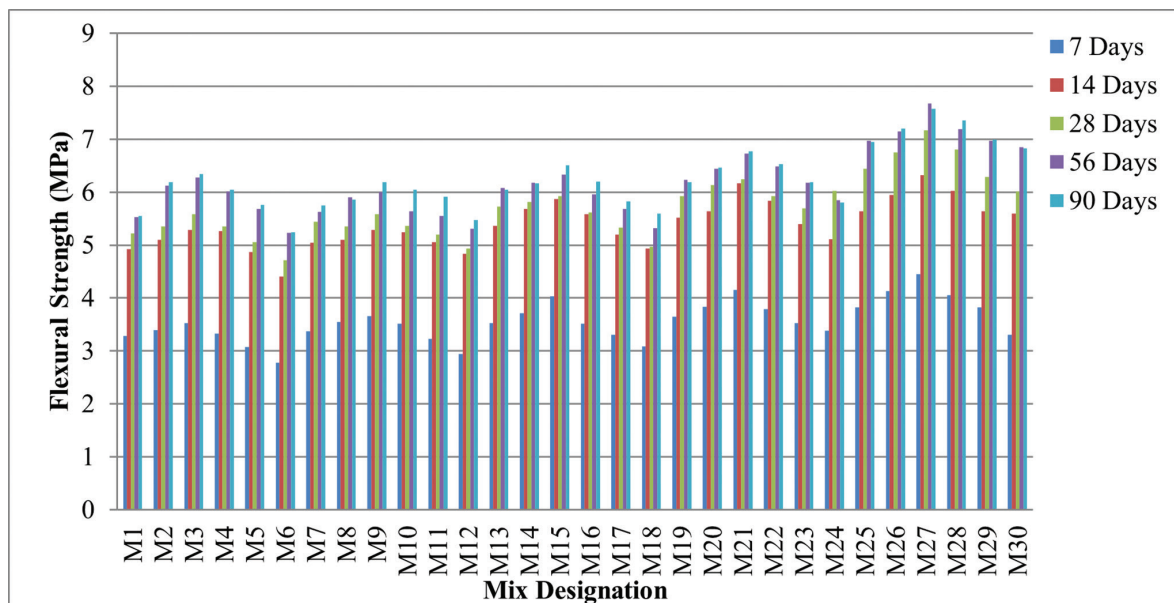


Figure 4: Graphical representation of split tensile strength variation from 7 to 90 days.

strength, while Table 8 lists the results of the test. The graphical depiction of the split tensile test results is shown in Figure 4 and the findings are presented in Table 9 and tabulated in Table 10. Figure 1 displays the test results for various samples' flexural strength [24, 25].

Mechanical properties show the optimum percentage of replacement is at M27 mix it is when the coconut shell and palm shell is replaced at 5% and 5% with binder ratio of 0.6 and molarity is 16. For M27 mix durability and microstructure investigation is done [22–25]. The durability properties are studied for the mix M25 conventional concrete (molarity 16 and binder ratio 0.6) and M27 (molarity 16 and binder ratio 0.6 with 5% of coconut shell and 5% of palm shell). The durability studies are carried out as shown in Figure 5.



**Table 10:** Flexural Strength behaviour of concrete from 7 to 90 days.

| MIX ID     | FLEXURAL STRENGTH @ 28 DAYS (N/mm <sup>2</sup> ) |             |             |             |               |
|------------|--|-------------|-------------|-------------|---------------|
|            | 7 DAYS   | 14 DAYS     | 28 DAYS     | 56 DAYS     | 90 DAYS       |
| M1         | 3.28   | 4.92        | 5.22        | 5.53        | 5.5469        |
| M2         | 3.40   | 5.10        | 5.35        | 6.12        | 6.1857        |
| M3         | 3.53   | 5.29        | 5.58        | 6.28        | 6.3462        |
| M4         | 3.33   | 5.26        | 5.35        | 6.01        | 6.0476        |
| M5         | 3.08   | 4.87        | 5.06        | 5.68        | 5.7603        |
| M6         | 2.78   | 4.41        | 4.72        | 5.23        | 5.2435        |
| M7         | 3.37   | 5.05        | 5.44        | 5.63        | 5.7523        |
| M8         | 3.55   | 5.10        | 5.35        | 5.90        | 5.8647        |
| M9         | 3.66   | 5.29        | 5.58        | 6.00        | 6.1857        |
| M10        | 3.52   | 5.24        | 5.36        | 5.64        | 6.0492        |
| M11        | 3.23   | 5.06        | 5.20        | 5.55        | 5.9176        |
| M12        | 2.94   | 4.84        | 4.94        | 5.31        | 5.4779        |
| M13        | 3.53   | 5.36        | 5.73        | 6.08        | 6.0412        |
| M14        | 3.71   | 5.68        | 5.82        | 6.18        | 6.1664        |
| M15        | 4.03   | 5.87        | 5.92        | 6.33        | 6.5051        |
| M16        | 3.52   | 5.58        | 5.62        | 5.96        | 6.2017        |
| M17        | 3.31   | 5.20        | 5.33        | 5.68        | 5.8245        |
| M18        | 3.09   | 4.94        | 4.97        | 5.32        | 5.5918        |
| M19        | 3.65   | 5.52        | 5.93        | 6.23        | 6.1841        |
| M20        | 3.84   | 5.64        | 6.13        | 6.44        | 6.4665        |
| M21        | 4.15   | 6.17        | 6.24        | 6.73        | 6.7715        |
| M22        | 3.79   | 5.84        | 5.93        | 6.49        | 6.5275        |
| M23        | 3.53   | 5.40        | 5.69        | 6.18        | 6.1857        |
| M24        | 3.38   | 5.11        | 6.02        | 5.85        | 5.8085        |
| M25        | 3.82   | 5.64        | 6.44        | 6.97        | 6.9464        |
| M26        | 4.13   | 5.95        | 6.75        | 7.15        | 7.2048        |
| <b>M27</b> | <b>4.45</b>                                      | <b>6.32</b> | <b>7.17</b> | <b>7.68</b> | <b>7.5804</b> |
| M28        | 4.05   | 6.02        | 6.80        | 7.19        | 7.3605        |
| M29        | 3.82   | 5.64        | 6.29        | 6.97        | 6.9946        |
| M30        | 3.31   | 5.60        | 6.01        | 6.85        | 6.8309        |

In this experimental work, specimens with dimensions of 150 × 150 × 150 mm were examined for compressive strength. A Compressive Testing Machine (CTM) with the capacity of 1000 KN was employed in this inquiry in accordance with IS: 516-1959. The samples are produced in accordance with the instructions, and the compressive strength is determined using the formula  $f_{ck} = P/A$ . The average values from three trials are reported in a table. where A is the cross - section area of a cube specimen in mm, P is the failure load in N, and  $f_{ck}$  is the compressive strength in N/mm<sup>2</sup>. As per IS 5816:1998, a test for split tensile strength was performed. Concrete specimens with a 150 mm diameter and 300 mm height were cast, and their split tensile strength was measured using a compression testing machine at the age of 7, 14, and 28 days (CTM). The samples are prepared in accordance with the instructions, and the average values for the first three trials are listed in a table. Compressive strength is determined using the formula  $2P/(dl)$ , where  $f_{ck}$  is the tensile strength in N/mm<sup>2</sup>, P is the failure load in N, d is the diameter of a cylinder specimen in mm, and l is the specimen's length in mm. A 100 mm × 100 mm × 500 mm prism was tested for flexural strength using a Universal Testing Machine (UTM) under single point loading conditions in accordance with IS: 516-1959 at the ages of 3, 7, 14, and 28 days. Figure 4 depicts the experimental configuration for flexural strength test. Equation  $PL/bd^2$  is used to compute the flexural strength. where b is the specimen's width in millimetres and d is the specimen's depth at the point of failure, L is the specimen's length in millimetres. P is maximum load in N on the specimen, where  $L = L/2$ .



Figure 5: Durability properties variation from 7 to 90 days.

According to calculations comparing water absorption of mixture M25 and M27, M27 has a higher saturation absorption than M25. At 28 days of cure, M25 absorbs saturated water at a rate of 5.87% and M27 at a rate of 6.04%. At 56 days of cure, M25 had a saturated water absorption rate of 4.96% and M27 of 5.18%. Due to the presence of palm and coconut shells, water absorption is slightly greater. The sample is submerged in  $H_2SO_4$  for 28, 56, and 90 days to determine the resistance to acid of M25 and M27. Weight loss with M27 is less pronounced than for M25 mix. M25 and M27 experienced weight loss of 1.12% and 0.66%, respectively, at an average age of 28 days. For M25 and M27, the percent of loss of weight at 56 days is 1.14% and 0.72%, respectively. For M25 and M27, the percentage of loss of weight at 90 days is 1.28% and 1.79%, respectively [26]. The sample is submerged in  $Na_2SO_4$  for 28, 56, and 90 days to determine the sulphate resistance for mixes M25 and M27. Weight loss with M27 is less pronounced than for M25 mix. M25 and M27 experienced weight loss of 1.18% and 0.67%, respectively, at an average age of 28 days. For M25 and M27, the percentage of loss of weight at 56 days is 1.16% and 0.79%, respectively. For M25 and M27, the percentage for weight loss at 90 days is 1.12% and 0.76%, respectively. At ages of 28 days as well as 56 days, the carbonation depths of the M25 as well as M27 mixes are computed. At the ages of 28 days and 56 days, M25 and M27's carbonation depths are 5.42 mm with 5.04 mm, respectively, and 6.24 mm and 6.52 mm, respectively. By conducting water permeability tests for 28 days and 56 days, the water permeability for mixes M25 and M27 is estimated. The weight loss for M27 is more than that with M27. Due to the use of coconut and palm shells at 5% and 5%, respectively, the water permeability in M27 is low [27–31].

#### 4. CONCLUSIONS

The following are the conclusions obtained based on the experimental research of mechanical properties, durability properties of hardened concrete: The 28-day compressive strengths were higher for concrete with coconut shell and palm ash at 5% and 5% replacement, the highest strength is obtained at mix M27 as 46.28 MPa at 28 days of compression strength when compare to conventional mix M25. The increase in percentage of compression strength is due to the presence of coconut shell and palm shell with molarity of 16. As the molarity increases the viscosity of concrete increases which leads to high strength. The 28-days tensile strength and flexural strength is more in mix M27 compare to the all-other mixes where in the increase in tensile and flexural strength are 2.36MPa and 2.72MPa at 5% CS and 5% PS replacement in conventional geopolymer mix. The durability study explains that the water absorption is more in M27 more due to coconut shell and palm shell compare to conventional concrete. Acid and sulphate resistance shows satisfactory results compare to conventional concrete. The optimum replacement is identified as M27 mix which is a geopolymer concrete where the coarse aggregate is replaced 5% with coconut shell and 5% palm shell with molarity of 16M. hence it is identified that this organic solid waste can be effectively replaced in concrete. As coconut shell aggregate has good impact resistance also the study is further will be extended for impact and bond characteristics.

#### 5. BIBLIOGRAPHY

- [1] Abdul Aleem M.I. and Arumairaj P.D. (2012), "Optimum Mix for the Geopolymer Concrete", International Journal of Science and Technology, V. 5, No. 3, pp 2299–2301.
- [2] Alengaram, U.J., Jumaat, M.Z., Mahmud, H. & Fayyadh, M.M., (2011), 'Shear behaviour of reinforced palm kernel shell concrete beams', Construction and building materials, v.25, no.6, pp. 2918–2927 <https://doi.org/10.1016/j.conbuildmat.2010.12.032>

- [3] Alengaram, U.J., Mahmud, H., Jumaat, M.Z. & Shirazi, (2010), 'Effect of aggregate size and proportion on strength properties of oil palm shell concrete', *International Journal of Physics Science*, v.5, no. 12, pp. 1848–56.
- [4] Aminul Islam Laskar and Rajan Bhattacharjee, (2012), "Effect of Plasticizer and Superplasticizer on Workability of Fly Ash Based Geopolymer Concrete", *International Conference on Advances in Architecture and Civil Engineering*, V.2. pp1–9.
- [5] Ganesh Prabhu, G., Arjunan, A., Samundeeswari, R., Arul Sivanantham, P., George Gabriel Vimal., A, Mukesh, P., Balamurugan, P., Vivek, S., Butsawan, B. (2023), Effects of fly ash and silica fume on alkalinity, strength and planting characteristics of vegetation porous concrete. *Journal of Materials research and technology*, 24, pp. 5347–5360
- [6] Gunasekaran, K., Ramasubramani, R., Annadurai, R. & Chandar, (SP 2014), 'Study on reinforced light-weight coconut shell concrete beam behavior under torsion', *Material and Design*, vol. 57, pp. 374–382 <https://doi.org/10.1016/j.matdes.2013.12.058>
- [7] Guo, X., Shi, H. & Dick, W.A., (2010), 'Compressive strength and microstructural characteristics of class C fly ash geopolymer', *Cement and Concrete Composites*, vol. 32, no. 2, pp. 142–147. <https://doi.org/10.1016/j.cemconcomp.2009.11.003>
- [8] Hardjito, D., Wallah, S.E., Sumajouw, D.M. & Rangan, B.V. (2004), "On the development of fly ash-based geopolymer concrete", *ACI Materials Journal-American Concrete Institute*, vol. 101, no. 6, pp. 467–72.
- [9] IS 10262-2009, "Recommended Guidelines for Concrete Mix Design", Bureau of Indian Standards, New Delhi, India.
- [10] IS 2386: Part- I, Methods of Test for Aggregates for Concrete, Bureau of Indian standards, New Delhi, 1963.
- [11] IS 383: Specification for Coarse and Fine Aggregates from Natural Sources for Concrete, Bureau of Indian standards, New Delhi, 1970.
- [12] IS 456: "Indian Standard Code for Plain and Reinforced Concrete, Code of practice, 4th Revision, BIS, New Delhi, 2000.
- [13] IS 516: "Method of Test for Strength of Concrete", Reaffirmed 2004, Bureau of Indian standards, New Delhi, 1959.
- [14] IS 9103: Specifications for Concrete admixtures Bureau of Indian standards, New Delhi, 1987.
- [15] Jayaprithika, A. & Sekar, S.K. (2016), 'Mechanical and fracture characteristics of Eco-friendly concrete produced using coconut shell, ground granulated blast furnace slag and manufactured sand', *Construction and Building Materials*, vol. 103, pp. 1–7. <https://doi.org/10.1016/j.conbuildmat.2015.11.035>
- [16] Joshi, S. & Kadu, M. (2012), 'Role of Alkaline Activator in Development of Eco-friendly Fly Ash Based Geo Polymer Concrete', *International Journal of Environmental Science and Development*, vol. 3, no. 5, pp. 417–421.
- [17] Kalaivani, K., Gunasekaran, K., & Annadurai, R. (2022), Innovative sustainable coconut husk mortar for ferrocement infrastructure solution. *Innovative Infrastructure Solutions*, 7(1), 131. <https://doi.org/10.1007/s41062-021-00728-1>
- [18] Kumarasamy, K., Kandasamy, G., & Ramasamy, A. (2023), Elucidation of Microstructural and Mechanical Properties of Coconut Husk Mortar as a Sustainable Building Material for Ferrocement. *Sustainability*, 15(5), 3995. <https://doi.org/10.3390/su15053995>
- [19] Monita, O. & Hamid, N. (2012), 'Properties of fly ash geopolymer concrete designed by Taguchi method', *Materials and Design*, vol. 36, pp. 191–198. <https://doi.org/10.1016/j.matdes.2011.10.036>
- [20] Muthupandy, V., Chandrasekaran, P., Vivek, S., & Ganeshan, P. (2022), Concrete with sisal fibered geopolymer: a behavioral study. *Journal of Ceramic Processing Research*, 23, 6, pp. 912–919.
- [21] Ramasubramani, R., & Gunasekaran, K. (2022), Study on plastic shrinkage of coconut shell concrete slab made with M-sand. *Innovative Infrastructure Solutions*, 7, 1–8. <https://doi.org/10.1007/s41062-021-00614-w>
- [22] Ramasubramani, R., & Gunasekaran, K. (2022), Study on the Influence of Manufactured Sand on Deflection Characteristics of Coconut Shell Concrete Slab. In *Sustainable Construction Materials: Select Proceedings of ACMM 2021* (pp. 353–363). Springer Singapore. [https://doi.org/10.1007/978-981-16-6403-8\\_30](https://doi.org/10.1007/978-981-16-6403-8_30)

- [23] Ramasubramani, R., & Gunasekaran, K. (2022), Sustainable replacement materials for concrete production from renewable resources and waste on interfacial bond properties. *Innovative Infrastructure Solutions*, 7(4), 266. <https://doi.org/10.1007/s41062-022-00869-x>
- [24] Ramkumar, K.B., PR, K.R., & Gunasekaran, K. (2023), Performance of hybrid steel fiber-reinforced self-compacting concrete RC beam under flexure. *Engineering Science and Technology, an International Journal*, 42, 101432. <https://doi.org/10.1016/j.jestch.2023.101432>
- [25] Sharma, V., Chandra, S., Choudhary, R. (2010), “Characterization of Fly ash Bituminous Concrete Mixes, *Journal of Materials in Civil Engineering*, vol.22, 12, pp. 1209–1216. [https://doi.org/10.1061/\(ASCE\)MT.1943-5533.0000125](https://doi.org/10.1061/(ASCE)MT.1943-5533.0000125)
- [26] Subbaiah Ilamvazhuthi S. & Gopalakrishna G.V.T. (2013), “Performance of Geopolymer Concrete with Polypropylene Fibres”, *International Journal of Innovations in Engineering and Technology*, Vol. 3, No. 2, pp 148–155.
- [27] Sureshbabu, Y., Ganeshan, P., Raja, K., & Vivek, S. (2023), Performance and Emissions Parameters Optimization of Thermal Barrier Coated Engine Tested with Tamanu Blended Diesel Fuel: A Novel Emission Pollution-Preventive Approach. *Global NEST Journal*, 25(3), pp 78–86.
- [28] Thilagashanthi, T., Gunasekaran, K., & Satyanarayanan, K.S. (2022), Reduction of Pores and Water Absorption of Coconut Shell Aggregate on Treatments. In *Sustainable Construction Materials: Select Proceedings of ACMM 2021* (pp. 365–375). Springer Singapore. [https://doi.org/10.1007/978-981-16-6403-8\\_31](https://doi.org/10.1007/978-981-16-6403-8_31)
- [29] Thirukumar, T., Krishnapriya, S., Priya, V., Sagai Francis, B., Anandhalakshmi, R., Dinesh, S., Poomalai, R., Vivek, S., & Saravanan, S. (2023), Utilizing rice husk ash as a bio-waste material in geopolymer composites with aluminium oxide. *Global NEST Journal*, <https://doi.org/10.30955/gnj.004694>
- [30] Verapathran, M., Vivek, S., Arunkumar, G.E., Dhavashankaran, D. (2023), Flexural behaviour of HPC beams with steel slag aggregate. *Journal of Ceramic Processing Research*, 24, 1, pp 89–97
- [31] Wani, F.A., & Gunasekaran, K. (2022), Study on the effects of composite concrete bifurcating the neutral axis without reinforcement. *Materials Today: Proceedings*, 68, 156–163. <https://doi.org/10.1016/j.matpr.2022.09.519>